ORGANIC CHEMISTRY

Organocatalyst-controlled stereoselective head-to-tail macrocyclizations

Jonas W. Rackl, Linus B. Boll, Helma Wennemers*

Chiral macrocycles are key to the discovery of new medicines. Their synthesis is, however, challenging and typically requires the often-cumbersome installation of stereochemical features in a linear precursor. In this study, we report a catalyst-controlled stereoselective head-to-tail macrocyclization. The method utilizes a bifunctional peptide catalyst to template the terminal functional groups of the linear precursor, thereby favoring intra- over intermolecular reaction and enabling exquisite control over the stereochemistry of the emerging stereogenic centers. Diverse 12- to 18-membered macrocyclic lactones and lactams were obtained from achiral linear precursors. The organocatalyst even dictates the stereochemical outcome upon cyclizing a chiral linear precursor. This catalyst-controlled stereoselective head-to-tail macrocyclization provides a practical route to chiral macrocycles with predictable stereochemical outcomes. The utility was highlighted by synthesizing the core of the natural product robotnikinin.

Macrocycles—molecules consisting of rings with 12 or more atoms—are widespread in nature and widely used in the biological, chemical, and material sciences (*1*–*3*). For medicine development, engineered macrocycles with one or more stereogenic centers open new therapeutic avenues (*4*–*6*). The efficient synthesis of such chiral macrocycles is, however, challenging (*7*–*12*). A key difficulty arises when converting a flexible linear precursor into a macrocyclic product because reducing the degrees of conformational freedom while introducing torsional and transannular strain favors intermolecular reactions (Fig. 1A) (*13*, *14*). Templating or tethering of terminal functional groups by a stoichiometric reagent or catalyst can favor macrocyclization (*12*, *15*–*21*). A second challenge is the controlled installation of one or more stereogenic centers upon macrocyclization (Fig. 1B). So far, stereoselective head-to-tail macrocyclizations have generally relied on embedded stereogenic centers in the linear precursor (*22*, *23*). The stereochemical bias embedded in the linear precursor is relayed to the newly established stereogenic centers, either through conformational preorganization, coordination to a catalyst or stoichiometric reagent, or a combination of both (Fig. 1C) (*22*–*26*). This strategy, however, often lacks a predictable stereochemical outcome and requires, in many cases, cumbersome syntheses of stereochemically defined linear substrates. Control over the configuration of one or more stereogenic centers upon macrocyclization of an achiral linear precursor streamlines the synthesis of chiral macrocycles (*27*, *28*). A stereoselective head-to-tail macrocyclization of an achiral substrate, however, has remained a formidable undertaking. In an ideal stereoselective macrocyclization, a catalyst controls the configuration of newly formed stereogenic centers, at best even overriding preexisting stereochemical bias in the linear precursor.

We envisioned that a tailored catalyst bearing an appropriate chiral spacer with functional groups for reaction or coordination with terminal functional moieties of the substrate could overcome the dual challenges of mitigating the thermodynamic penalties associated with macrocyclization and controlling the stereochemistry at the emerging stereogenic center(s) (Fig. 1, D and E). Ideally, such a stereoselective macrocyclization catalyst would be easily accessible, metal-free, and environmentally benign.

We chose the conjugate addition between an aldehyde and a ketovinyl ester as a testing ground for a catalyst-controlled, stereoselective macrocyclization (Fig. 1E). This reaction yields macrolides—macrocyclic lactones that are prevalent structural motives in natural products (*7*)—with keto and aldehyde functionalities as versatile moieties for downstream derivatization. We envisioned a chiral bifunctional organocatalyst bearing an amine and an H-bond donor to activate the substrate through covalent enamine formation and to preorganize the substrate for macrocyclization by a noncovalent interaction between the H-bond donor and the vinyl ketoester (Fig. 1E). Compound **S1**, bearing an aldehyde moiety and a vinyl ketoester attached to an alkyl chain, served as a model substrate for translating this blueprint into a synthetic methodology (Fig. 2). This conjugate addition yields through C–C bond formation two stereogenic centers at the ring closure site and, if successful, utilizes a readily available, benign organocatalyst.

Reaction development

We commenced by assessing the reactivity of linear precursor **S1** in the presence of different secondary amine-based organocatalysts (Fig. 2) (*29*). The catalysts encompassed amines lacking a proton donor and others featuring an intramolecular proton donor. Attempts to promote the macrocyclization using pyrrolidine (**A**) and diarylprolinol silyl ether **B**, a popular organocatalyst for related intermolecular reactions (*30*, *31*), converted γ-ketoester aldehyde **S1** (25 mM) only to a small extent (<10% consumption), regardless of solvent, the presence or absence of acetic acid, or other reaction parameters (Fig. 2, entries 1 to 3). By contrast, proline (**C**) (*32*), featuring a secondary amine and a COOH group, facilitated greater but still limited consumption of **S1** (<30% conversion with 10 or 20 mol % of **C** within 18 hours at room temperature; Fig. 2, entry 4). The reaction yielded macrocycle **1** and, to a slightly greater extent, dimer **1′** resulting from intermolecular reaction (**1:1′** = 0.8:1). This result suggests that the combination of an amine and an intramolecular COOH group is important for reactivity. Peptide H-D-Pro-Pro-Glu-NH_2, **D1** (*33*, *34*), a catalyst featuring these groups in a β-turn conformation with an intramolecular salt bridge (*35*), proved much more effective than proline. Complete substrate conversion to the 16-membered macrocycle **1** and the dimer **1′** (**1:1′** = 2.4:1) took place within 18 hours at room temperature (Fig. 2, entry 5). Catalysts lacking a COOH group (**D2**) did not convert linear precursor **S1**, corroborating the importance of a bifunctional catalyst with an intramolecular proton donor (Fig. 2, entry 6). Tripeptide **D1** formed macrocycle **1** with exquisite enantioselectivity [99% enantiomeric excess (ee)] and a diastereomeric ratio (d.r.) of 2:1 (*syn*/*anti*) at a catalyst loading of 10 mol %. Building on these results, we optimized the reaction conditions of the macrocyclization by variations of the catalyst, substrate concentration, and other common reaction parameters, such as the reaction time, catalyst loading, and solvent (tables S2 and S3). These trials identified tripeptide H-D-Pro-$^{\alpha}$MePro-Glu-NH_2 (**D3**) (*36*) as the most effective catalyst enabling both high yield and excellent stereoselectivity. Using 3 mol % of **D3** in $CHCl_3$:*i*-PrOH (9:1) at a substrate concentration of 2.5 mM **S1** afforded within 18 hours at room temperature the 16-membered macrocycle **1** in 97% yield with an enantioselectivity of 99% ee and a diastereomeric ratio exceeding 20:1 (Fig. 2, entry 8, and Fig. 3A). Dimer **1′** formed under these conditions only in small amounts with a macrocycle-to-dimer ratio of 37:1 (**1:1′**). In ethyl acetate, a "greener" solvent alternative, macrocycle **1** formed in the presence of 3 mol % of **D1** still with high efficiency [**1:1′** = 9.2:1, d.r. = 11:1, 98% ee; table S3].

Laboratory of Organic Chemistry, Department of Chemistry and Applied Biosciences (D-CHAB), ETH Zürich, Zürich, Switzerland. *Corresponding author. Email: helma.wennemers@org.chem.ethz.ch

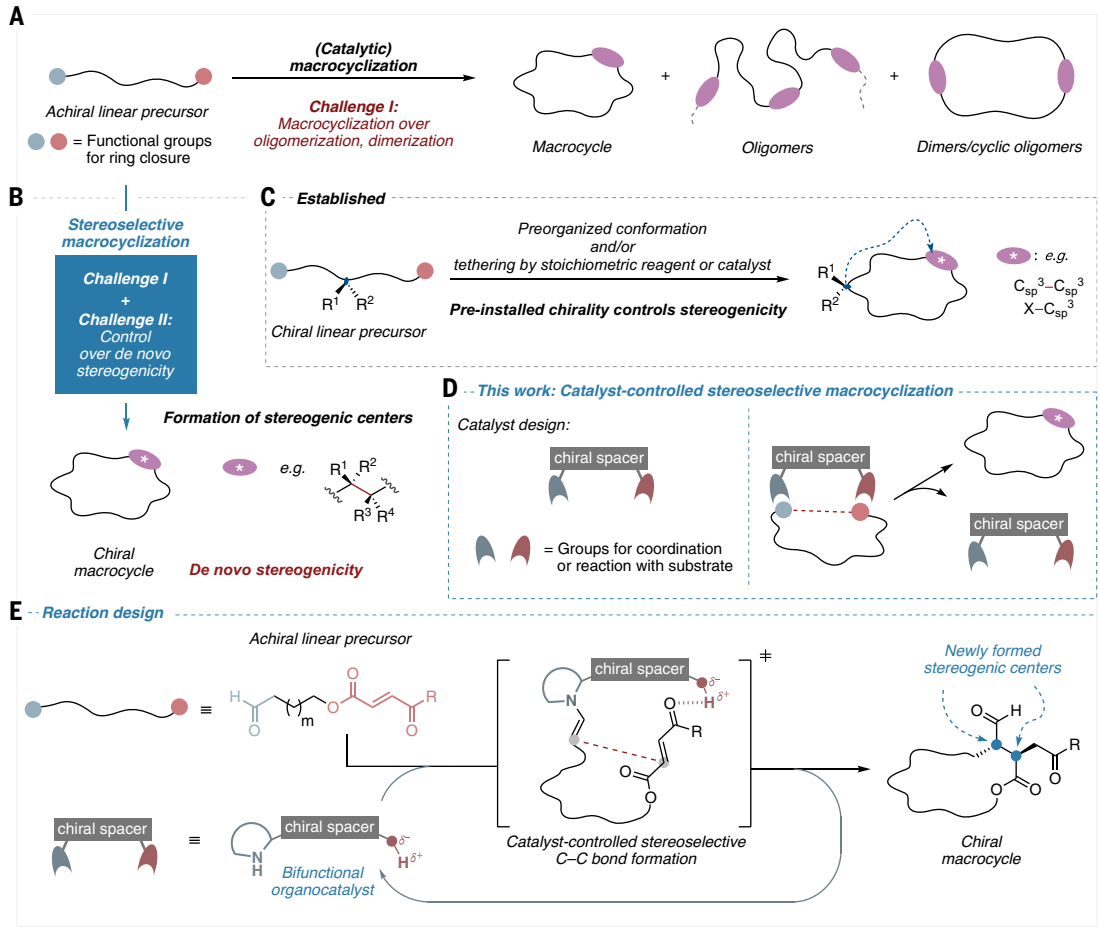

Fig. 1. Challenges of catalytic macrocyclization and reaction design. (**A**) Challenges for (catalytic) macrocyclizations to form achiral products. (**B**) Dual challenges for stereoselective head-to-tail macrocyclization. (**C**) Relay of stereochemical information upon macrocyclization of a chiral linear precursor. (**D**) General catalyst design for stereoselective head-to-tail macrocyclizations. (**E**) Envisioned organocatalyst-controlled stereoselective macrocyclization.

Ring-size variations and stereochemical model

With optimized reaction parameters identified, we evaluated the chemical space accessible through this peptide-catalyzed stereoselective macrocyclization. Variations of the length of the alkyl chain between the aldehyde and the vinyl ketoester showed that the peptide catalyst forms macrocycles ranging from 12- to 18-membered rings with high yields and stereoselectivities (Fig. 3A). Each macrocyclization proceeded with a diastereoselectivity exceeding 20:1 and the major *syn* diastereoisomer formed with near-perfect enantioselectivity (99% ee). For the ring sizes ≥13, the macrocycle-to-dimer ratio was >20:1, with very high macrocyclization yields of 92 to 97% (Fig. 3A). The 12-membered macrocycle **2** formed with the lowest macrocycle-to-dimer ratio (3.5:1) and yield (78%).

The data are consistent with tethering of the substrate by the peptide catalyst through enamine formation and H-bonding to the vinyl ketoester in a conformation conducive to intramolecular, stereoselective bond formation (Fig. 3B). The stereochemical outcome of the macrocyclization is in accordance with a nucleophilic approach of an s-*trans*, *E*-configured enamine intermediate onto the *E*-configured γ-ketoester moiety. Following Seebach's topological rule (*37*), this *Re*/*Re* facial reaction affords the experimentally observed (*S*,*R*)-configuration at the newly formed stereogenic centers (Fig. 3B).

A closer inspection of the data shows that the selectivity for macrocyclization over competing dimerization increased with the size of the macrocycle (Fig. 3C). The 16-membered ring formed with the highest selectivity (**1**:**1**′ = 37:1) and the 12-membered ring with the lowest (**2**:dimers = 3.5:1). This trend suggests that a rising enthalpic penalty associated with torsional and transannular strain in the macrocyclic products renders the organocatalyzed macrocyclization more challenging for smaller rings. Thus, we evaluated the ring strain computationally. Following a density functional theory workflow described by Houk and James (*38*), ring strains were estimated by relating enthalpies of hydrogenation of the macrocycles to those of a linear analog (fig. S3). We found an inverse correlation between the macrocycle-to-dimer ratio and the calculated ring strain (Fig. 3C). This finding corroborates a rising enthalpic penalty of macrocyclization for the formation of smaller rings. Expansion of the ring size from a 16-membered to an 18-membered macrocycle (**5**) slightly decreased the selectivity for macrocyclization (**5**:dimers = 25:1), despite a predicted lower ring strain. We reason that, once ring strain is diminished, the increased conformational flexibility of the linear substrate lowers the effective molarity of the reactive termini and, thus, favors inter- over intramolecular pathways.

Functional group compatibility and macrocycle derivatizations

Next, we explored the compatibility of the organocatalytic stereoselective macrocyclization with various functional groups at the Michael acceptor and within the ring (Fig. 4A). We focused on substrates that challenge our methodology with regard to reactivity and stereoselectivity rather than enumerating close analogs (*39*). Substituents of vinyl ketones influence the reactivity of this electrophile. Macrolides from

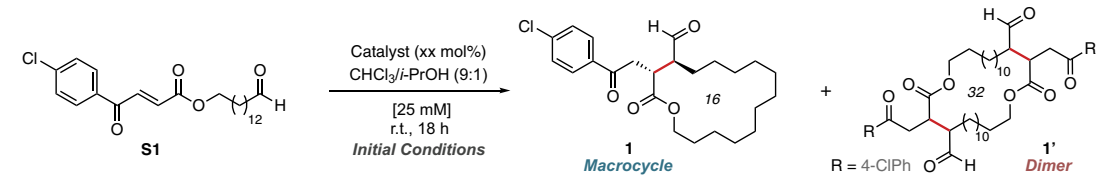

Entry	Catalyst	x mol%	Variation from initial conditions	Consumption *S1**	Ratio* *1:1'*	d.r.*	ee†
1	**A**	20	none	<5%	n.d.	n.d.	n.d.
2	**B**	20	Toluene, 20 mol% AcOH	<10%	n.d.	n.d.	n.d.
3	**B**	20	MeOH, 20 mol% AcOH	<10%	n.d.	n.d.	n.d.
4	**C**	20	none	29%	0.8:1	5:1	33%
5	**D1**	10	none	*quant.*	2.4:1	2:1	99%
6	**D2**	20	none	<5%	n.d.	n.d.	n.d.
7	**D1**	3	2.5 mM	*quant.*	10:1	>20:1	99%
8	**D3**	3	2.5 mM	*quant.*	37:1	>20:1	99%

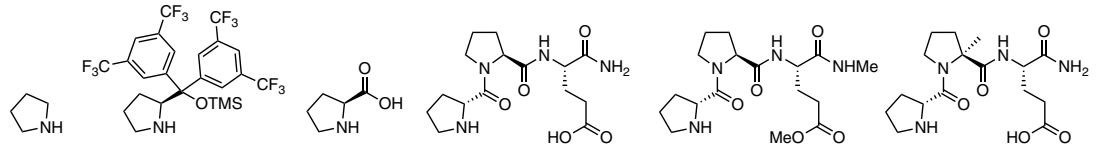

Fig. 2. Reaction optimization for the organocatalyzed stereoselective macrocyclization. The peptide catalysts were used as trifluoroacetic acid (TFA) salts with an equimolar amount of *N*-methylmorpholine (NMM). Control experiments showed that the TFA•NMM salt does not affect the catalysis (table S3). *Determined by proton nuclear magnetic resonance (^{1}H-NMR) spectroscopy of the crude reaction mixture. †ee of isolated product **1** was determined by high-performance liquid chromatography (HPLC) on a chiral stationary phase. n.d., not determined; r.t., room temperature.

reactions with analogs bearing electron-rich and electron-poor aromatic substituents [dioxymethylene (**6**) and *p*-trifluoromethyl (**7**), respectively] formed in 93 to 96% yield, with diastereomeric ratios up to 20:1 and excellent enantioselectivity (99% ee). An *o*-methoxy substituent (**8**), which reduces the electrophilicity of the Michael acceptor, was similarly compatible (88% yield, 99% ee, d.r. >20:1). Even a considerably less-reactive aliphatic cyclopropyl vinyl ketone (**9**) underwent cyclization with high yield (81%) and stereoselectivity (d.r. = 10:1, 99% ee). Substrates bearing catechol (**10**) and alkyne (**11**) moieties formed macrocycles in yields >95% with 99% ee and d.r. >20:1. The efficient formation of **10** and **11** is notable because the incorporation of sp^2- and sp-hybridized carbons could be expected to exacerbate angle strain owing to deviations from ideal bond angles. Calculated lowest-energy conformers feature, however, near-ideal bond angles, which is consistent with negligible angle strain (fig. S4B). In addition, the reduced number of hydrogen atoms diminishes torsional and transannular contributions to ring strain, as manifested by low calculated ring strain (1.8 and 1.5 kcal/mol, respectively; fig. S3). Recognizing the prominence of lactams among macrocyclic natural products and pharmaceuticals (*5*), we replaced the vinyl ketoester with an analogous amide (**12**), a substitution that modifies the electronic properties of the Michael acceptor substantially and introduces potential competing H-bonding interactions with the peptide catalyst. The respective macrocyclization proceeded with excellent diastereoselectivity (d.r. >20:1), yield (96%), and enantioselectivity (99% ee). Even a macrocycle bearing amide and ester bonds (**13**) formed in the presence of the peptide catalyst with outstanding selectivity (93% yield, 95% ee, d.r. >20:1). These results highlight the robustness of the peptide-catalyzed macrocyclization to altered Michael acceptors and moieties in the linear precursor that could engage in noncovalent interactions, e.g., H-bonding (*40*), and thus, interfere with interactions between the substrate and the tripeptide critical to catalysis.

We envisioned the aldehyde moiety within the macrocycles as a versatile handle for downstream functionalizations to engraft further structure and function onto the macrocyclic scaffold (Fig. 4B). Indeed, subjecting model macrocycle **9** to hydrazone formation provided ligated product **14** in quantitative yield (99% ee, d.r. = 10:1). Oxidation of the aldehyde to carboxylic acid **15** proceeded smoothly and allowed for subsequent coupling with an amino acid derivative to yield macrocycle **16**. This example illustrates how the macrocyclic scaffolds could be conjugated to biomolecules, e.g., peptides and proteins, offering an avenue to, e.g., dual targeting (*41*). Macrocycle **1** also proved amenable to excision of the formyl group. The Rh-mediated decarbonylation yielded the structurally simpler, yet synthetically challenging α-substituted macrolactone **17**. Traditional methods for obtaining such macrolactones rely on Baeyer-Villiger oxidation followed by alkylation, a route that requires harsh conditions and does not allow for stereocontrol (*42*).

Catalyst-controlled macrocyclization of a chiral linear precursor

Lastly, we assessed the capacity of the bifunctional peptide catalyst to accommodate potentially biasing stereochemical features of the linear precursor during macrocyclization and still control the configuration of the stereogenic centers emerging from the ring-closing C–C bond formation. To explore such a catalyst-controlled macrocyclization, we used linear precursor **S18** bearing a ketovinyl amide acceptor and an ester moiety with a phenyl group at an adjacent (*R*)-configured stereogenic center. In the presence of 3 mol % of peptide **D3**, the respective 12-membered macrocycle **18a** with (*S*,*R*)-configuration at the new stereogenic centers was obtained in 93% yield with excellent stereoselectivity (>20:1 d.r., >99% ee; Fig. 5, right). This is a notable result, in particular considering that the macrocycle contains only 12 atoms and features, therefore, more ring strain than larger analogs. Emerging

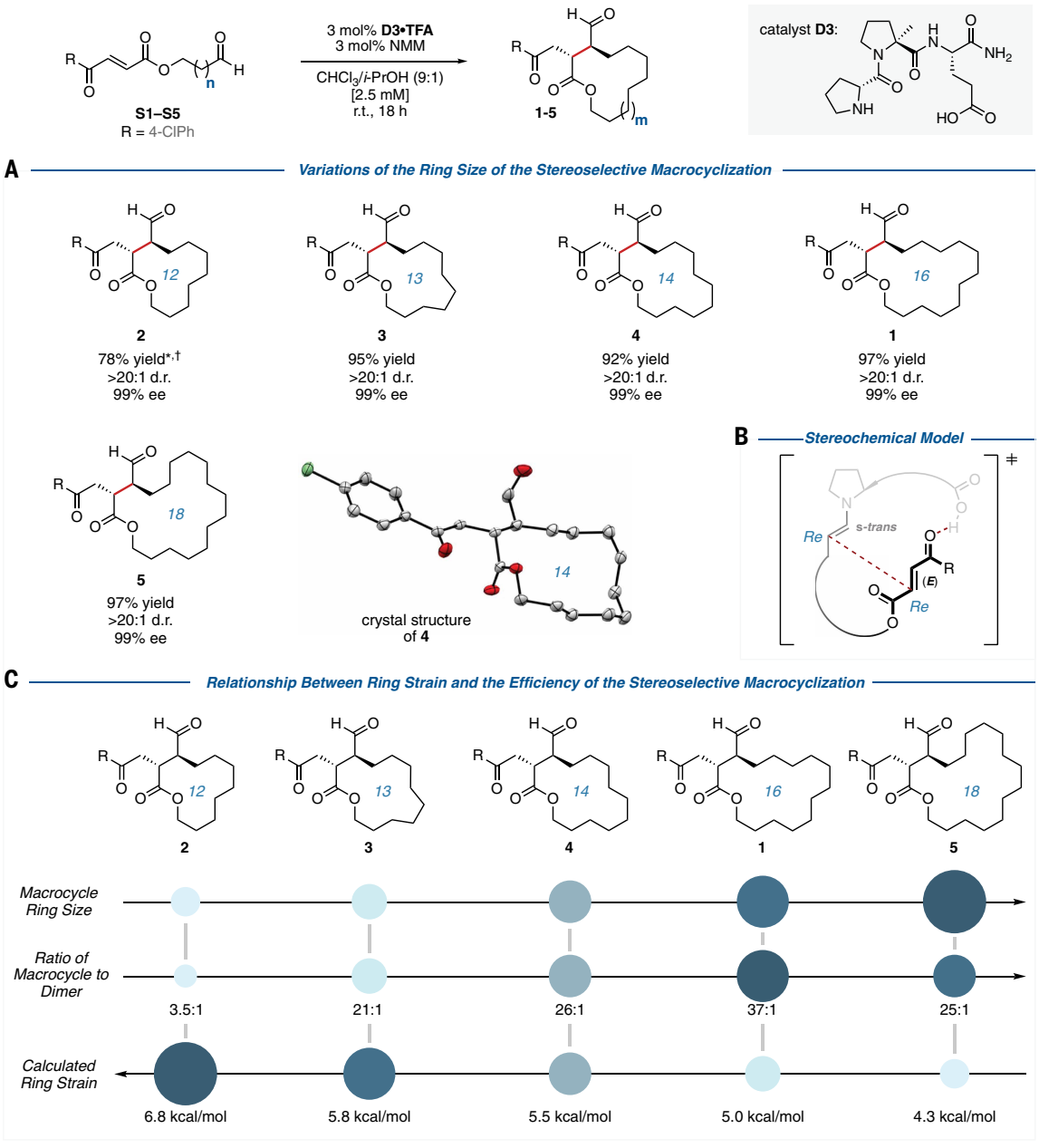

Fig. 3. Influence of ring size and strain on the peptide-catalyzed stereoselective macrocyclization. (**A**) Macrocycles with different ring sizes. Yields refer to isolated macrocycles. Diastereoselectivity (d.r.) and ee were determined as listed in Fig. 2. *Reaction time, 72 hours. †Yield of *syn*-diastereoisomer. (**B**) Stereochemical model. The s-*trans*, *E*-configured enamine intermediate undergoes *syn*-selective intramolecular conjugate addition to the *E*-configured γ-ketoester through a *Re*/*Re* approach. (**C**) Relationship between ring strain and efficiency of macrocycle formation. Ring strains were estimated from enthalpies of hydrogenation of the macrocycles and a linear analog using a workflow described in (*38*) at the B3LYP-D3/def2-TZVP[CPCM($CHCl_3$)] level of theory using ORCA (fig. S3).

ring strain could be compensated for by a favorable positioning of the reactive groups during the cyclization through the stereogenic center in the linear precursor. The combination of the (*R*)-configured substrate with peptide **D3** could, thus, be a "match," whereas the combination with the enantiomer of the catalyst could be a "mismatch" with the substrate. To evaluate the degree of catalyst control, we combined (*R*)-configured **S18** with the enantiomer of the peptide catalyst (*ent*-**D1**) under otherwise identical conditions (because the enantiomer of $^{\alpha}$MePro is not easily accessible, we used the enantiomer of peptide **D1**). Notably, this reaction provided the diastereoisomeric macrocycle **18b** with (*R*,*S*)-configuration at the newly formed stereogenic centers in 92% yield and essentially perfect stereoselectivity (>20:1 d.r., >99% ee; Fig. 5, left). These results demonstrate that the macrocyclization proceeds with full control over the stereochemical induction by the peptide catalyst, regardless of preexisting stereochemical information. From a practical standpoint, such catalyst-controlled macrocyclizations are highly desirable for accessing enantiomeric as well as diastereoisomeric macrocycles from a single linear precursor. The approach circumvents the need for often cumbersome syntheses of enantiomeric or diastereoisomeric linear precursors to introduce stereochemical features into the macrocycle. Stereochemically divergent macrocyclizations are particularly appealing when catalyst enantiomers are readily

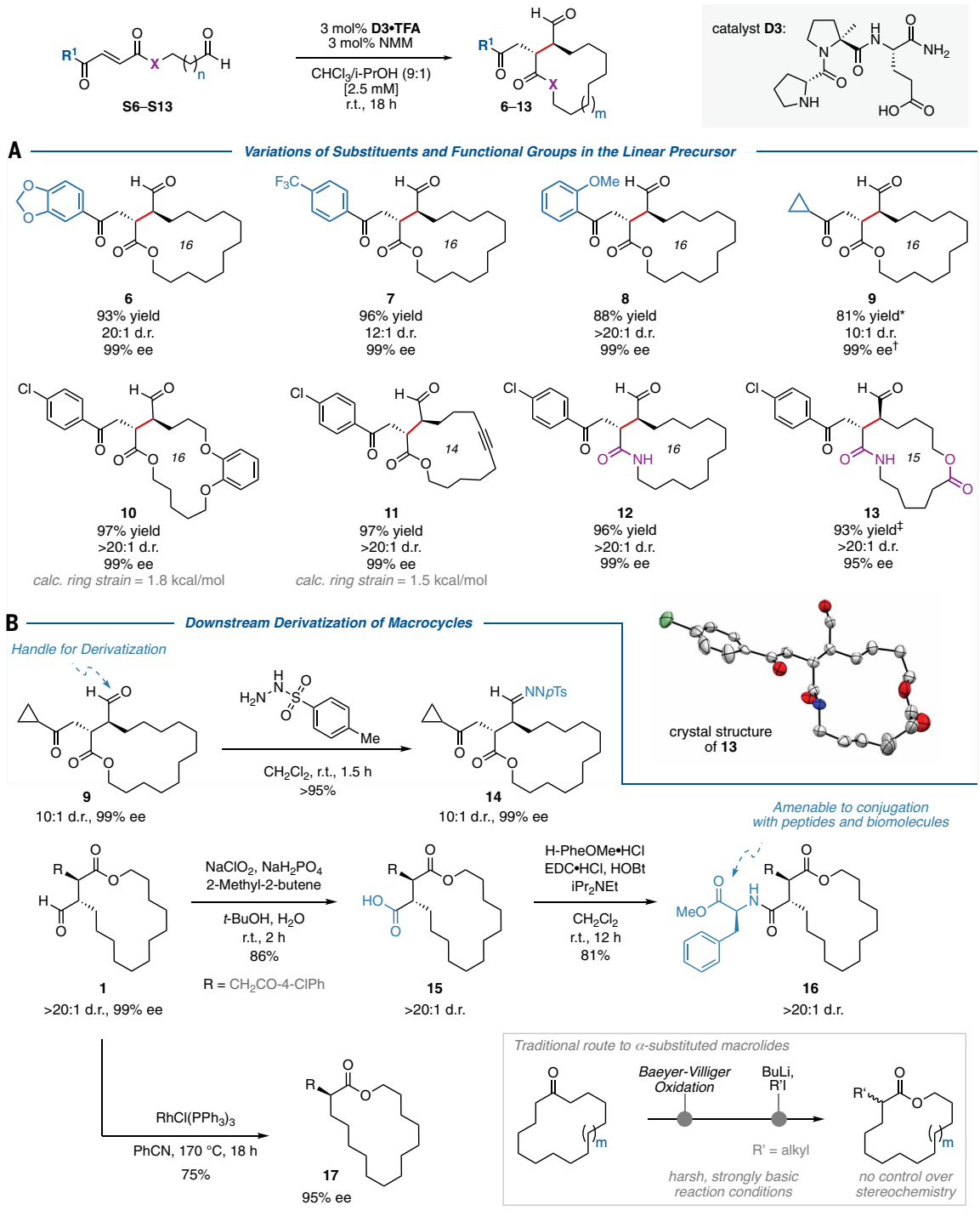

Fig. 4. Effect of substituents and functional groups in the linear precursor on the stereoselective macrocyclization and downstream derivatization. (**A**) Variations of substituents and functional groups in the linear precursor. Diastereoselectivity (d.r.) and ee were determined as listed in Fig. 2. *Reaction time, 21 days. †The ee was determined by analyzing hydrazone **14** on chiral stationary–phase HPLC. ‡Reaction time, 62 hours. (**B**) Examples of downstream derivatizations.

available and operate without altering the substrate or reaction conditions. Notably, macrocycle **18a** captures the robotnikinin core, a pharmacophore of therapeutic interest associated with selective binding to Sonic Hedgehog (Shh) protein (*43*), and maintains orthogonal sites for downstream diversification. Thus, our methodology offers a practical, stereodefined starting point for analog generation, enabling, e.g., structure-activity relationship studies on macrocycles of pharmaceutical interest.

Conclusions and outlook

We have addressed the long-standing challenge of stereoselective head-to-tail macrocyclizations by leveraging a bifunctional peptide catalyst. The organocatalyst engages the substrate dually, through covalent enamine formation and noncovalent H-bonding, effectively tethering the termini in a conformation conducive to intramolecular stereoselective bond formation. Our methodology robustly facilitates access to 12- to

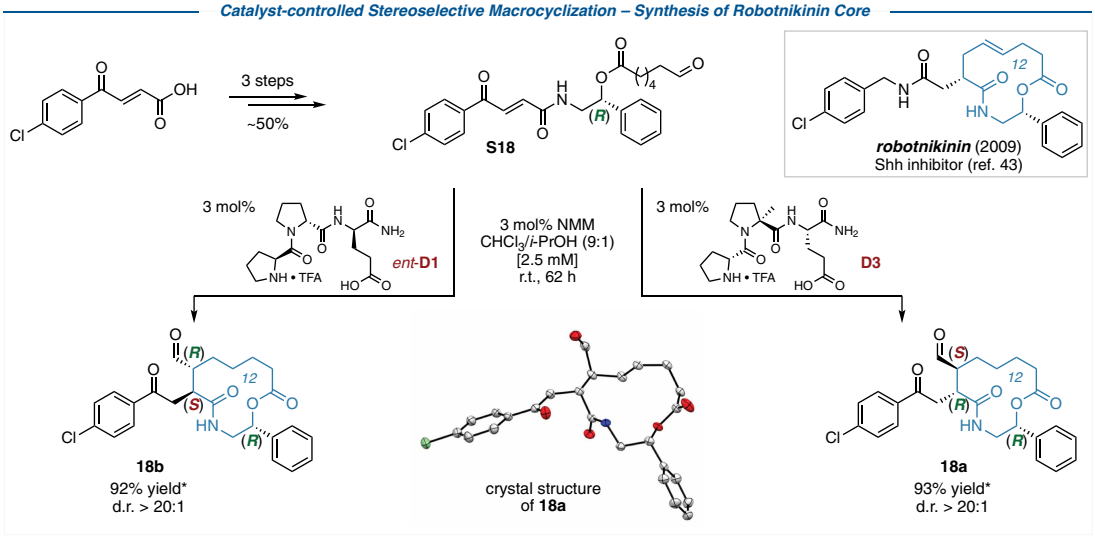

Fig. 5. Catalyst-controlled stereoselective macrocyclization of a chiral linear precursor. Access to diastereoisomers from a chiral linear precursor through use of enantiomeric peptide catalysts. The obtained macrolides feature the core of robotnikinin (*43*). *Yield of shown diastereoisomer.

18-membered macrocycles from diverse achiral substrates with exquisite control over the stereochemistry and competing intermolecular reactions. The organocatalyst dictates the stereochemical outcome of the macrocyclization irrespective of preexisting stereochemical features in the substrate. Both enantiomers of the peptide catalyst are readily accessible, enabling the synthesis of diastereoisomeric macrocycles from a single linear precursor. Combined, our methodology provides a practical route to chiral macrocycles with predictable stereochemical outcome, upgrading the synthetic toolbox for constructing molecules with beneficial properties in medicine and beyond. In a broader context, we anticipate our fundamental insights into the key prerequisites for effective catalysis will pave the way into a rich realm of catalyst-controlled stereoselective macrocyclizations.

REFERENCES AND NOTES

1. E. A. Villar *et al.*, *Nat. Chem. Biol.* **10**, 723–731 (2014).
2. A. K. Yudin, *Chem. Sci.* **6**, 30–49 (2015).
3. M. Jirásek, H. L. Anderson, M. D. Peeks, *Acc. Chem. Res.* **54**, 3241–3251 (2021).
4. D. Garcia Jimenez, V. Poongavanam, J. Kihlberg, *J. Med. Chem.* **66**, 5377–5396 (2023).
5. E. Marsault, M. L. Peterson, *J. Med. Chem.* **54**, 1961–2004 (2011).
6. D. J. Newman, G. M. Cragg, in *Macrocycles in Drug Discovery*, J. Levin, Ed., part of Drug Discovery Series (Royal Society of Chemistry, 2015), pp. 1–36.
7. A. Parenty, X. Moreau, G. Niel, J. M. Campagne, *Chem. Rev.* **113**, PR1–PR40 (2013).
8. T. Gulder, P. S. Baran, *Nat. Prod. Rep.* **29**, 899–934 (2012).
9. I. Saridakis, D. Kaiser, N. Maulide, *ACS Cent. Sci.* **6**, 1869–1889 (2020).
10. Y. Li, X. Yin, M. Dai, *Nat. Prod. Rep.* **34**, 1185–1192 (2017).
11. A. Fürstner, *Acc. Chem. Res.* **54**, 861–874 (2021).
12. V. Martí-Centelles, M. D. Pandey, M. I. Burguete, S. V. Luis, *Chem. Rev.* **115**, 8736–8834 (2015).
13. M. A. Casadei, C. Galli, L. Mandolini, *J. Am. Chem. Soc.* **106**, 1051–1056 (1984).
14. C. Galli, L. Mandolini, *Eur. J. Org. Chem.* **2000**, 3117–3125 (2000).
15. C. J. Pedersen, *J. Am. Chem. Soc.* **89**, 2495–2496 (1967).
16. F. Diederich, P. J. Stang, R. R. Tykwinski, Eds., *Modern Supramolecular Chemistry: Strategies for Macrocycle Synthesis* (Wiley-VCH, 2008).
17. R. H. Grubbs, S. J. Miller, G. C. Fu, *Acc. Chem. Res.* **28**, 446–452 (1995).
18. M. Yu *et al.*, *Nature* **479**, 88–93 (2011).
19. X. Shen *et al.*, *Nature* **541**, 380–385 (2017).
20. Z. C. Girvin, M. K. Andrews, X. Liu, S. H. Gellman, *Science* **366**, 1528–1531 (2019).
21. P. P. Lampkin, S. H. Gellman, *J. Am. Chem. Soc.* **147**, 3731–3739 (2025).
22. K. Zheng, R. Hong, *Nat. Prod. Rep.* **36**, 1546–1575 (2019).
23. K. Zheng, R. Hong, *J. Org. Chem.* **89**, 7355–7365 (2024).
24. W. C. Still, D. Mobilio, *J. Org. Chem.* **48**, 4785–4786 (1983).
25. C. M. Hayward, D. Yohannes, S. J. Danishefsky, *J. Am. Chem. Soc.* **115**, 9345–9346 (1993).
26. J. Hwang, B. Q. Mercado, S. J. Miller, *Proc. Natl. Acad. Sci. U.S.A.* **118**, e2113122118 (2021).
27. F. Panahi, B. Breit, *Angew. Chem. Int. Ed.* **63**, e202317981 (2024).
28. B.-L. Wang, J.-Q. Yu, Q. Zhang, X.-W. Wang, *JACS Au* **5**, 2159–2171 (2025).
29. S. Mukherjee, J. W. Yang, S. Hoffmann, B. List, *Chem. Rev.* **107**, 5471–5569 (2007).
30. Y. Hayashi, H. Gotoh, T. Hayashi, M. Shoji, *Angew. Chem. Int. Ed.* **44**, 4212–4215 (2005).
31. K. L. Jensen, G. Dickmeiss, H. Jiang, L. Albrecht, K. A. Jørgensen, *Acc. Chem. Res.* **45**, 248–264 (2012).
32. B. List, R. A. Lerner, C. F. Barbas III, *J. Am. Chem. Soc.* **122**, 2395–2396 (2000).
33. M. Wiesner, M. Neuburger, H. Wennemers, *Chemistry* **15**, 10103–10109 (2009).
34. M. Wiesner, J. D. Revell, S. Tonazzi, H. Wennemers, *J. Am. Chem. Soc.* **130**, 5610–5611 (2008).
35. C. Rigling *et al.*, *J. Am. Chem. Soc.* **140**, 10829–10838 (2018).
36. T. Schnitzer, J. W. Rackl, H. Wennemers, *Chem. Sci.* **13**, 8963–8967 (2022).
37. D. Seebach, J. Goliński, *Helv. Chim. Acta* **64**, 1413–1423 (1981).
38. A. R. Bogdan, S. V. Jerome, K. N. Houk, K. James, *J. Am. Chem. Soc.* **134**, 2127–2138 (2012).
39. M. C. Kozlowski, *Org. Lett.* **24**, 7247–7249 (2022).
40. A. G. Doyle, E. N. Jacobsen, *Chem. Rev.* **107**, 5713–5743 (2007).
41. C. J. Gerry, S. L. Schreiber, *Nat. Chem. Biol.* **16**, 369–378 (2020).
42. D. S. Clyne, L. Weiler, *Tetrahedron* **55**, 13659–13682 (1999).
43. B. Z. Stanton *et al.*, *Nat. Chem. Biol.* **5**, 154–156 (2009).
44. J. W. Rackl, L. B. Boll, H. Wennemers, Organocatalyst-controlled stereoselective macrocyclizations (Supplementary Materials), version v2, Zenodo (2025); https://doi.org/10.5281/zenodo.18153659.

ACKNOWLEDGMENTS

We are grateful to the Swiss National Science Foundation and ETH Zurich for financial support. L.B.B. is grateful to the Fonds der Chemischen Industrie (Germany) for a Kekulé Fellowship. We thank N. Trapp and M. Solar from the Small Molecule Crystallography Center (SMoCC) of ETH Zurich for recording the x-ray crystal structures. We thank E. Löher, L. Gautier, N. V. Shcherbakov and K. J. Patej (ETH Zurich) for synthetic contributions. **Funding:** This project received funding from the Swiss National Science Foundation (200020_219409/1, H.W. and R'Equip Project 206021_213224). **Author contributions:** J.W.R. and H.W. conceived the study. J.W.R. performed experiments and L.B.B. performed computational analyses. All authors contributed to data analysis. H.W. supervised the research and acquired funding. J.W.R., L.B.B., and H.W. wrote the manuscript. **Competing interests:** The authors declare that they have no competing interests. **Data, code, and materials availability:** Crystallographic parameters are freely available from the Cambridge Crystallographic Data Center (CCDC) under references CCDC 2471270 (**1**), 2471268 (**4**), 2471269 (**11**), and 2471267 (**16a**). Computational details, including conformer-rotamer ensembles after CREST and CENSO, geometries from ORCA runs, as well as further input and output files for each step of the workflow, are publicly accessible on Zenodo (*44*). All other data are available in the main text or the supplementary materials, as are details for the synthesis of all reported products.

SUPPLEMENTARY MATERIALS

science.org/doi/10.1126/science.aec8992
Materials and Methods; Supplementary Text; Figs. S1 to S5; Tables S1 to S8; References (*45*–*66*)

Submitted 7 October 2025; accepted 13 January 2026

10.1126/science.aec8992

Organocatalyst-controlled stereoselective head-to-tail macrocyclizations

Jonas W. Rackl, Linus B. Boll, and Helma Wennemers

Science **391** (6788), . DOI: 10.1126/science.aec8992

Editor's summary

A common strategy for producing large molecular rings is to first generate a linear precursor and then loop it back on itself with a favorable clasping reaction. Rackl *et al*. present an innovative catalyst for this type of loop closure in 12-to-18 membered rings: directing a conjugate addition between an aldehyde and a ketovinyl ester (see the Perspective by Dong and Zhao). The tripeptide catalyst selects for just one of two possible mirror image configurations at the linkage point, even overriding existing stereochemical bias in the precursor. —Jake S. Yeston

Science (ISSN 1095-9203) is published by the American Association for the Advancement of Science. 1200 New York Avenue NW, Washington, DC 20005. The title *Science* is a registered trademark of AAAS.